Film-forming amines for corrosion protection of carbon steels in PWR secondary circuit conditions

J. Baux, N. Pebere, S. Delaunay, J. Tireau, M. Roy, D. You, Jl. Bretelle

Film-forming amines for corrosion protection of carbon steels in PWR secondary circuit conditions

J. Baux[a,b], N. Pébère[a], S. Delaunay[b], J. Tireau[b], M. Roy[c], D. You[c], J.-L. Bretelle[d]

[a]*Université de Toulouse, CIRIMAT, UPS/INPT/CNRS*
ENSIACET, 4 allée Emile Monso, 31030 Toulouse Cedex 4, France.
[b]*EDF R&D / Materials and Mechanics of Components Department / Chemistry and Corrosion Group, Avenue des Renardières, 77818 Moret-sur-Loing Cedex, France.*
Den – Service d'Etude du Comportement des Radionucléides (SECR), CEA, Université Paris-Saclay, 91191, Gif-sur-Yvette, France
[d]*EDF / Power Generation Division, 1 Place Pleyel, 93200 Saint Denis, France*

Abstract

During layup periods of pressurized water reactors (PWRs), corrosion phenomena can affect metallic components of the secondary circuit, mainly carbon steel. The use of corrosion inhibitors such as film-forming amines (FFAs) is an interesting way to attenuate or stop these phenomena and extend the lifetime of the materials. Film-forming amines (FFA) have both a hydrophilic head which can adsorb on metal or oxides surface, and a hydrophobic tail which can organizes rather perpendicularly to the surface and create, by accumulation, a barrier between the metal and the corrosive environment.

The aim of the present work is to investigate the behavior and the efficiency of FFA for the carbon steels protection under various physical and chemical conditions, representative of the PWR secondary circuits. Carbon steel plates was submitted to treatment at temperatures between 120 °C and 275 °C in an autoclave with or without FFA: here the octadecylamine (ODA). The adsorption of the FFA and the corrosion inhibition efficiency of the films formed on the steel surface were characterized by contact angle measurements, scanning electron microscopy (SEM) and electrochemical impedance spectroscopy (EIS).

Introduction

During layup periods of PWRs for maintenance operation, corrosion phenomena can occur on carbon steel materials due to oxygen entrance. Use of alternative corrosion inhibitors such as film-forming amines (FFA) is a promising approach to reduce or to stop the corrosion of carbon steel, which constitute the major part of the PWR secondary circuit [1,2]. A key benefit of film-forming amines is to improve the corrosion protection during startups, shutdowns and layups of the PWR and, as a consequence, startup will be quicker, leading to significant economic repercussions [1]. Even though FFA have been used successfully for decades to treat boiler feed water in industrial power plants [3], their behavior and the physical characteristics of the film formed on the carbon steel surface are not well described. The FFA tested in this paper was octadecylamine (ODA), $CH_3(CH_2)_{17}NH_2$, a well-known corrosion inhibitor for steel in nuclear power plants and fossil fuel power plants for years [1,3–10].

First, this paper introduces a key characteristic of ODA which is the water/steam distribution coefficient. Then, the ODA deposition on carbon steel samples in representative thermo-chemical secondary circuit conditions was investigated. Surface morphology observations and contact angle measurements were supplemented by electrochemical analysis in order to assess the anti-corrosion efficiency of the film formed. Experimental devices and tests conditions were described. The obtained results were discussed in order to highlight the remaining gaps on FFA behavior understanding. The contact angle test, commonly used to state upon the formation of an FFA film on a metallic surface, was also discussed.

Chemical Composition and Action Mode of ODA

The ODA molecule is constituted by one aliphatic alkyl group (hydrophobic part) of 18 carbon atoms with one amine function (hydrophilic head). ODA has the simplest FFA structure. FFA molecules can adsorb on metal or oxide surfaces to form an insulating hydrophobic film, thus creating a barrier which limits the access of water and corrosive species (oxygen, carbon dioxide, chlorides…) toward the metal or metal oxide surface. The strong affinity of FFA for metal surfaces is due to the lone pair of electrons on nitrogen [11]. The mechanism of ODA adsorption could be physisorption or chemisorption, depending on physico-chemical parameters (temperature, pH…). The latter would lead to stronger bonds to the surface.

Experimental Part

Materials

The P275 low carbon steel was chosen as representative material of PWR. Its composition is reported in Table 1. The steel sample was machined to obtain small coupons (dimensions were 30x20x3 mm). Before the deposition step, the surface was wet ground with silicon carbides (SiC) papers down to grade 800, cleaned ultrasonically with ethanol, rinsed with deionized water and dried.

Table 1: Chemical composition of the P275 carbon steel (EN10028-3).

Element (wt%)	C	Si	Mn	Cr	Mo	Ni	Cu	Fe
P275 NL1	0.16	0.4	0.5-1.5	0.3	0.08	0.5	0.3	Bal.

ODA Deposition

The ODA deposition was performed in an autoclave (Figure 1) in representative conditions of the secondary circuit in static conditions. The autoclave was made of titanium. It contained a sampling hose, a temperature probe and a rotating axis to ensure a good homogeneity of the liquid phase. The rotation speed was fixed at 100 rotations per minute (rpm). Three carbon steel plates were placed in the mesh and two at the bottom of the autoclave to evaluate the reproducibility.

The solution was chemically conditioned a $pH_{25\ °C}$ between 9.6 and 9.8 with ethanolamine (ETA) and ammonia (NH_3). The media was deaerated with nitrogen bubbling during 10 min before each experiment. Hydrazine was added to ensure a complete deaeration (reducing conditions). For security reasons, the autoclave was not completely filled with the solution. A steam phase was present above the liquid solutions.

The effect of ODA was studied at 120 °C, 220 °C and 275 °C. To be consistent with site conditions, the samples treated at 120 °C and 220 °C were immersed in the liquid phase. And

those treated at 275 °C were placed in the steam side. The ODA concentration in the liquid phase was controlled to be close to 2 mg/kg (maximum aimed concentration for ODA based conservation).

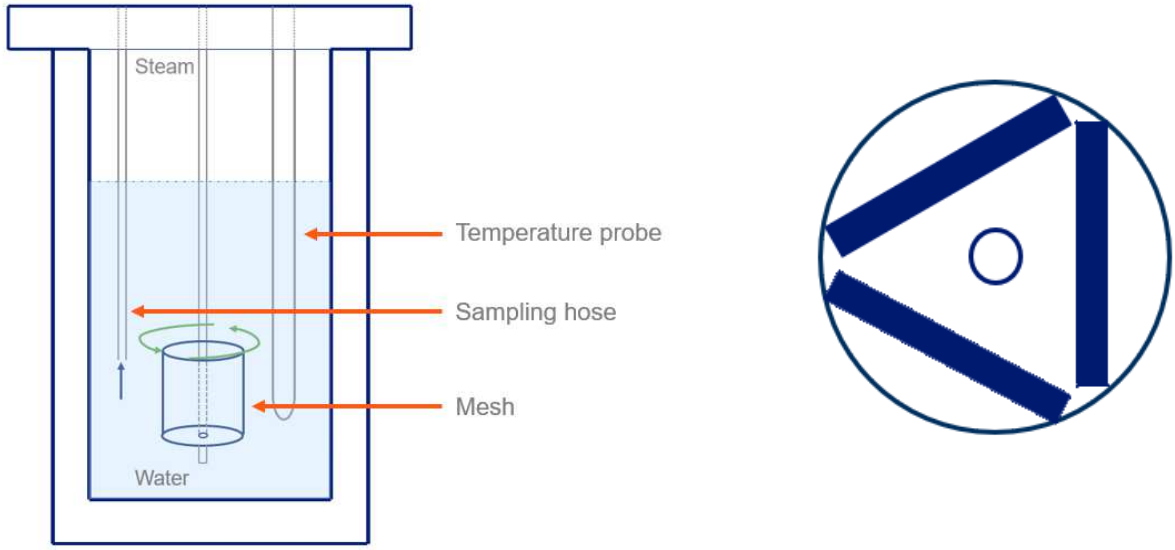

Figure 1: Schematic representation of the autoclave used to simulate the secondary circuit thermo-chemical conditions (left). Schematic representation of the mesh with the three carbon steel plates (right).

Surface Characterizations

Optical observations were performed with a binocular loupe and an Olympus PMG3 optical microscope. The contact angles were measured using a Krüss Mobile Surface Analyze. The protocol consisted in depositing a deionized water drop of an accurate volume of 1 µL on the sample surface (bare metallic surface or treated surface with ODA) and then measuring the static contact angle (θ) 60 s after the deposition. The contact angle value was obtained by calculating the slope of the tangent to the drop at the liquid-solid interface thanks to the Advance software. To assess the homogeneity of the surface properties, 20 measurements were performed on different locations on the samples surface and the average contact angle was calculated with the standard deviation. All the experiments were performed at room temperature.

Electrochemical Measurements

The electrochemical cell used was a Bio-Logic® three electrodes cell with a saturated sulfate reference electrode and a platinum grid as counter electrode. The working electrode consisted of the carbon steel plate. Electrochemical impedance measurements were performed using a Solartron 1286 electrochemical interface connected to a Solartron 1250 frequency response analyzer. Impedance diagrams were obtained under potentiostatic regulation at the corrosion potential (E_{corr}) in the frequency range of 65 kHz to 10 mHz with 8 points per decade, using a 15 mV_{rms} sinusoidal voltage. Impedance data beyond 6.5 kHz were not taking into account due to experimental artifacts. Data modeling was carried out using the SimAd software developed at the LISE CNRS (Paris). The electrolyte solution was prepared from analytical grade Na_2SO_4 10^{-3} M and deionized water in equilibrium with air ($[O_2]_{25\,°C}$ = 8 mg/kg). $pH_{25\,°C}$ was adjusted at 9.6 – 9.8 with NH_3 and ETA. The choice of this medium was based upon its low electrical conductivity, close to that encountered in industrial water circuit, its low corrosiveness toward carbon steel and because it is an easily reproducible baseline solution.

Results and Interpretation

Water/Steam Distribution Coefficient of ODA

Preliminary experiments were performed to determine apparent water/steam distribution coefficient of ODA at 120, 220 and 275 °C. As a steam phase was always present in the autoclave during the tests, the ODA behavior according to the different tested temperatures was a key parameter to foresee its concentration both in the liquid and the steam phase. The desired ODA concentration in the liquid phase during the deposition close to 2 mg/kg.

To determine the ODA distribution coefficient, the following methodology was used:

1 – Preparation of a concentrated ODA solution (50 mg/kg)
2 – Performing sampling and ODA analysis at the tested temperature in the liquid phase
3 – Deducing the ODA concentration in the steam phase and calculation of the apparent distribution coefficient.

The hypothesis of a negligible adsorption of the ODA on the autoclave surfaces was made based on the following calculation: assuming that one ODA molecule occupies 20 Å² [12], 0.72 µg ODA was calculated to cover the inner surface of the autoclave (320 cm²) and considering a monolayer. This quantity is negligible compared to the injected mass of ODA (12.5 mg), even in the case of the formation of a multilayer film. We can conclude that the lost ODA is mainly due to the distribution of ODA between the liquid and the steam phase and not to adsorption on the autoclave surface.

The determined distribution coefficient of ODA for the different tested temperatures are presented in Figure 2 and compared to literature data [13].

As it can be seen, the experimentally calculated ODA distribution coefficients are close to those theoretically determined, especially at 220 °C. The coefficients determined at 120 °C and 275 °C, even if they follow the same trend of the curve, show a sufficient difference that makes it non-suitable to directly use the curve from literature for the concentration prediction of ODA in the liquid phase.

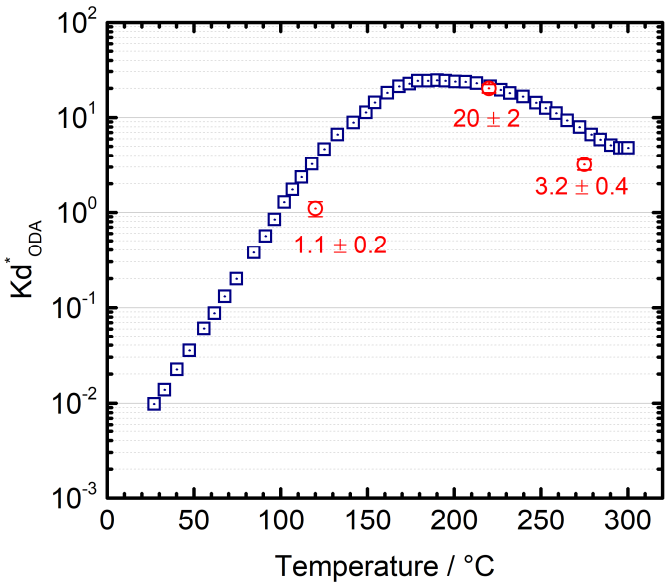

Figure 2: Water/steam ODA distribution coefficient as a function of the temperature (in red the present study, in blue Ramminger et al. [13]). The uncertainty of the calculated coefficient was due to the dosage protocol of ODA by spectrophotometry UV/Vis.

Influence of Temperature on Surface Oxides Formed and Hydrophobicity

The SEM images of the surface morphology of the coupons treated at different temperatures with and without ODA, are shown in Figure 3. The morphology of the samples shows the formation of a typical magnetite oxide layer for all the coupons. Dark areas are visible on the samples treated at 120 °C and at 220 °C (Figure 3.b and 3.d). Their composition, qualitatively determined by EDX (Figure 4), highlights an enrichment in carbon in the dark areas. The deposited crystal size is clearly larger for the samples treated at 275 °C (Figure 3.e and 3.f) even for a short period of time (2 h). Dark, ODA-rich areas could not be seen for this sample. The contact angle measured for the ODA treated samples at 120 °C (Figure 3.a and 3.b) and at 220 °C (Figure 3.c and 3.d) show a significant change in the surface hydrophobicity attributed to the ODA adsorption. In fact, the contact angle increases by about 22° and 25° for the treated ODA carbon steel at 120 °C and 220 °C respectiveley compared to their reference samples. The contact angle for the sample treated with ODA at 275 °C in the steam phase (Figure 3.f) does not change significantly (≈ 14°) compared to the reference sample (Figure 3.e) even though a better hydrophobic character can be noticed. In this case, the surface roughness seems to play a significant role in the contact angle measurement.

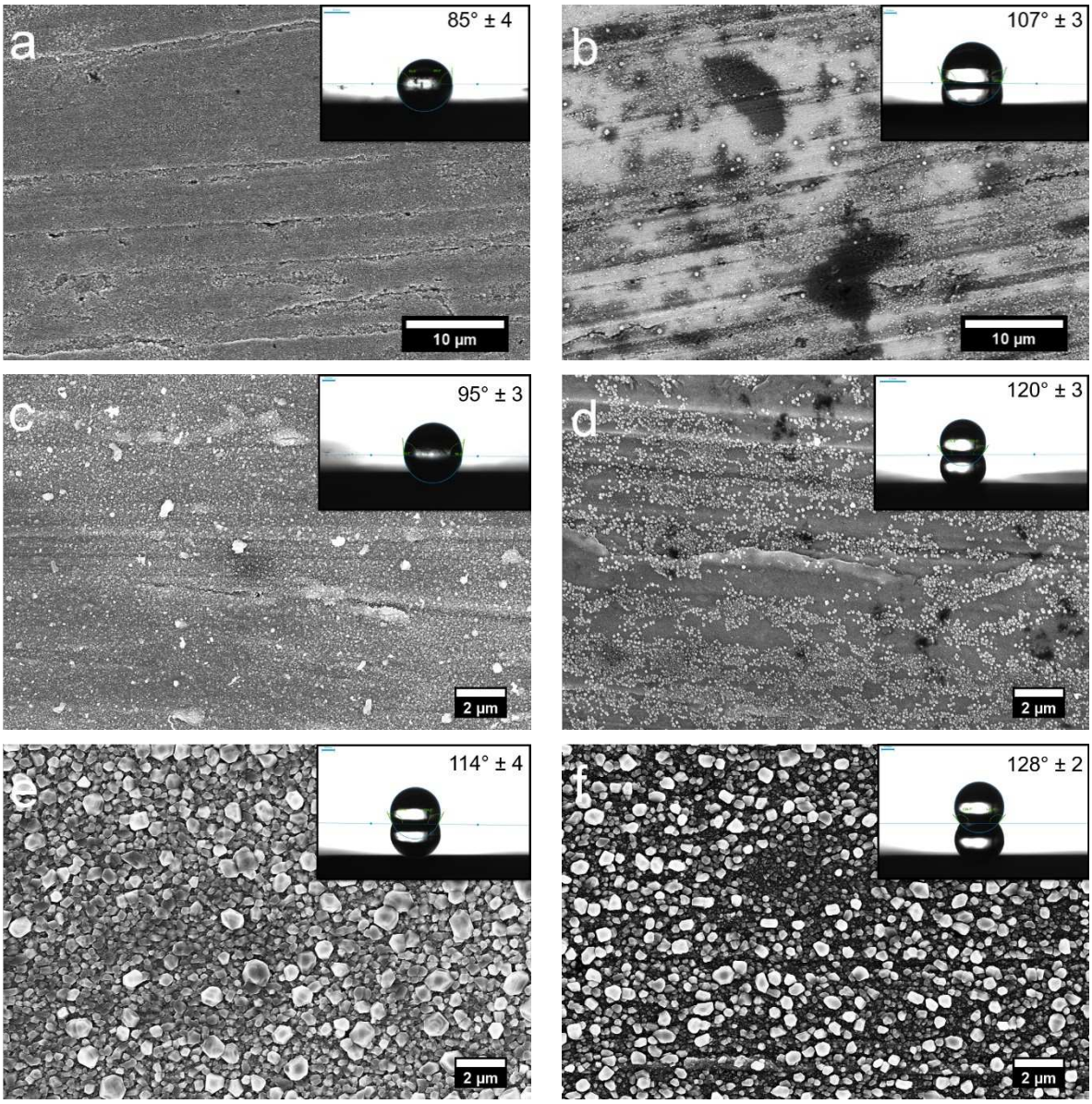

Figure 3: Surface morphologies of the carbon steel samples observed by SEM after treatments in the autoclave at a) 120 °C during 168 h without ODA, b) 120 °C during 168 h with 2 mg/kg ODA. c) 168 h at 220 °C without ODA, d) 168 h at 220 °C with 2 mg/kg ODA. e) 2 h at 275 °C in the steam without ODA, f) 2 h at 275 °C in the steam with 2 mg/kg ODA (concentration in the liquid phase).

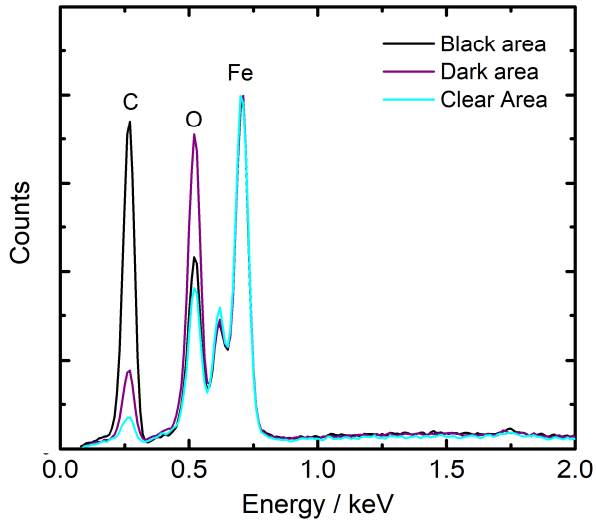

Figure 4: EDX spectra (normalized from the Fe peak) corresponding to different areas on the treated ODA carbon steel at 120 °C during 168 h (figure 3.b).

Influence of the Temperature on ODA Deposition and Efficiency

Figure 5 presents the impedance diagrams obtained for the carbon steel treated with 2 mg/kg of ODA during one week at 120 °C. This deposition time was necessary for such a low ODA concentration and has been determined from previous experiments. The impedance diagram of the treated carbon steel sample was compared with a blank obtained in the same conditions without ODA. The impedance modulus (Figure 5.a) at low frequency (10^{-3} Hz), was considered as a measure of the instantaneous corrosion resistance. A significant increase of the modulus after treatment with ODA (more than two decades) is observed. The phase angle (Figure 5.b) shows, at high frequency, a constant-phase element (CPE) behavior (phase angle lower than -90 degrees) which can be associated to the presence of a dielectric film (e.g. ODA film) on the working electrode surface. This time-constant is not visible on the blank sample. The origin of the CPE behavior can be attributed to an in-depth resistivity gradient in the film [14,15]. Therefore, the high frequency impedance data can be regressed by a power-law model (Eq. 1). Then, the physical parameters of the ODA film can be extracted (*e.g.* the thickness and the permittivity) (Figure 6), according to our previous results [16]. The regressed parameters are reported in table 2.

$$Z(\omega) = \delta \int_0^1 \frac{1}{\frac{1}{\rho_0} + j\omega\varepsilon\varepsilon_0 + \left(\frac{1}{\rho_\delta} - \frac{1}{\rho_0}\right)\xi^\gamma} d\xi \qquad \text{(Eq. 1)}$$

Where:
- δ is the ODA film thickness;
- ε is the ODA film permittivity;
- ε_0 is the permittivity of vacuum;
- ω is the pulsation;
- ρ_0 and ρ_δ are the resistivity at the metal/film interface and film/electrolyte interface, respectively;
- ξ is the dimensionless position;
- γ is a parameter indicating the variation of the resistivity.

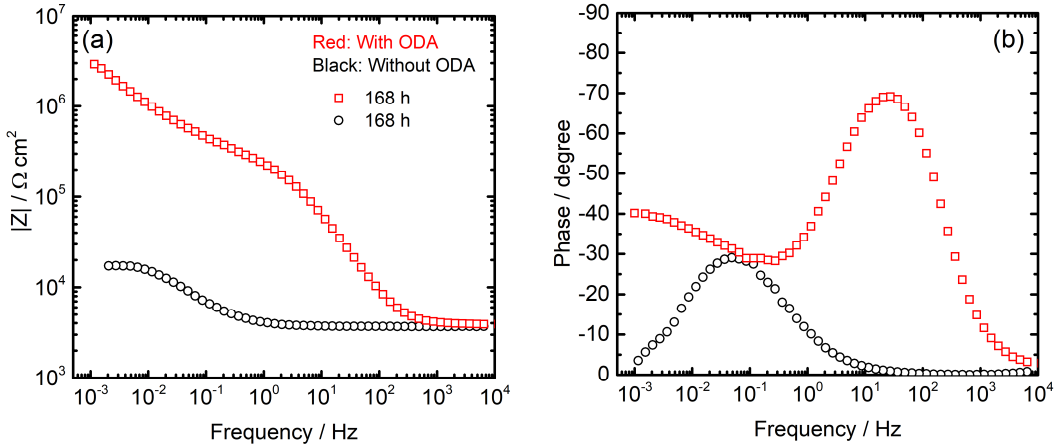

Figure 5: Impedance diagrams in Bode coordinates of the carbon steel treated samples at 120 °C during 168 h with 2 mg/kg ODA (red) and without ODA (black). (a) Impedance modulus and (b) phase angle.

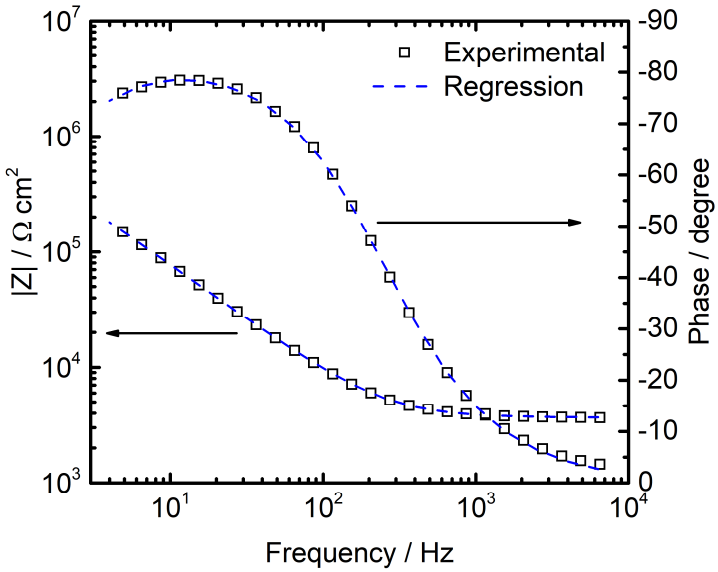

Figure 6: Impedance diagram of the carbon steel ODA treated sample at 120 °C during 168 h with 2 mg/kg ODA fitted with the power-law model in the frequency range corresponding to the electrochemical response of the film.

Table 2: Values of the regressed parameters with the power-law model. Comparison with literature data and graphical analysis.

Power-law parameters	Regressed parameters	
δ (nm)	18 ± 2	From graphical analysis: 18 ± 5
γ	20 ± 1	From graphical analysis: 20
ε	2.8 ± 0.1	From literature [17]: 2.7

Figure 7 shows the impedance diagrams of the carbon steel treated samples with and without ODA at 220 °C during 168 h. In this case, the impedance magnitude difference between the treated and untreated samples is modest compared to what have been observed for treatment at 120 °C. This is in accordance with the SEM observations showing scarce dark areas at the surface of the carbon steel treated with ODA at 220 °C. Besides, the presence of organic molecules on the surface was corroborated by drop angle measurements showing a significant improvement of the hydrophobicity of the treated ODA sample's surface (Figure 3.c and 3.d). However, data fitting was not possible in this case due to the poor definition of the film related time-constant. This could mean that the ODA film wasn't dense enough leading to weak anti-corrosive properties. A thermal degradation of ODA during the treatment at 220 °C could explain the poor film quality.

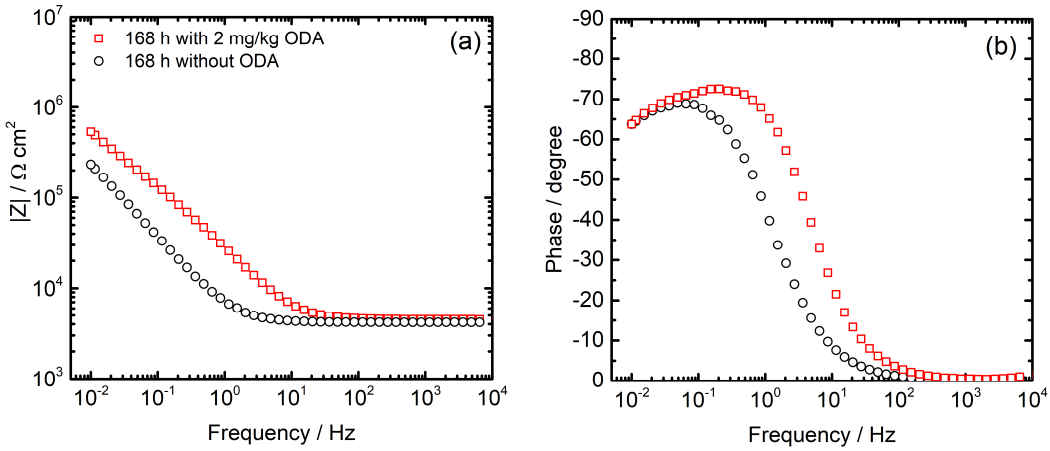

Figure 7: Impedance diagrams in Bode coordinates of the carbon steel treated samples at 220 °C during 168 h with 2 mg/kg ODA (red) and without ODA (black). (a) Impedance modulus and (b) phase angle.

The ODA concentration in the liquid phase at 275 °C was followed during 24 hours (Fig. 8). The dosage of ODA highlights a rapid diminution of the ODA concentration (80%) in less than 6 hours at 275 °C. After 24 hours the ODA concentration is almost zero. The main hypothesis to explain this result was a thermal degradation of ODA in a period of time comprised between 2 and 24 hours at 275 °C

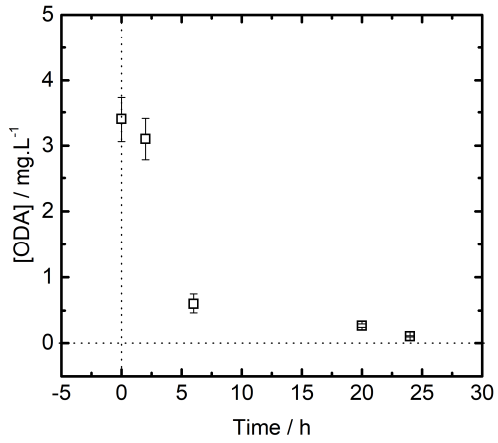

Figure 8: Evolution with time of the ODA concentration in the liquid phase at 275 °C.

Figure 9 shows a comparison of Bode plots resulted for carbon steel after treatment at 275 °C after 2 hours with 2 mg/kg ODA and without ODA, and after 24 hours with ODA. The impedance magnitude shows a significant increase after 2 hours with ODA compared to the reference sample. Besides, two time-constants are visible on the phase after 2 hours of treatment with ODA, although there is not well-defined phase rotation related to the film. The impedance magnitude decreases between 2 hours and 24 hours. The phase shows only one time constant, meaning that the response of the film disappears after 24 hours at 275 °C, in accordance with the decreasing concentration of ODA.

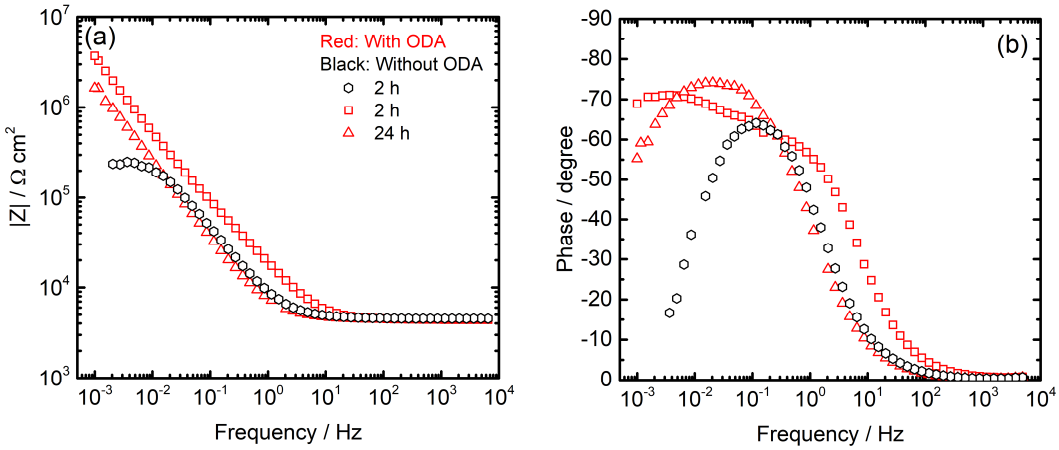

Figure 9: Impedance diagrams in Bode coordinates of the carbon steel treated samples at 275 °C in the steam phase during 2 h and 24 h with 2 mg/kg ODA (red) and during 2 h without ODA (black). (a) Impedance modulus and (b) phase angle.

Discussion

First, it was seen in Figure 2 that the distribution coefficient of ODA is a key parameter that must be taken into account in order to control the ODA concentration in the two phases (water or steam). At high temperature, ODA has a pronounce affinity for the steam phase that can lead to a decrease of the ODA concentration in water and an over-concentration of ODA in the steam.

The surface observations coupled with contact angle and EIS measurements clearly revealed the presence of an ODA film on the surface of the carbon steel sample at 120 °C and seem to indicate the presence of ODA on the surface of the sample treated at 220 °C. A better hydrophobicity was highlighted as well as a higher impedance modulus at low frequency. However, the corrosion protection of the treated surfaces could not always be linked to the measure of the contact angle as the surface roughness also played a role in the hydrophobic character of the surface, particularly in the case of the carbon steel treated at 275 °C with or without ODA. In that case, the contact angle did not increase significantly after the ODA deposition. Therefore, the contact angle measurement is a qualitative way to follow the variation of the hydrophobicity of a surface but it does not allow the phenomenon responsible of this hydrophobicity (organic film or surface roughness) to be discriminated. A link between hydrophobicity and anti-corrosive properties cannot clearly be established.

The quantification of ODA along time and EIS measurements after 2 h and 24 h of treatment with ODA at 275 °C showed that ODA degraded almost completely in few hours in water

conditioned at $pH_{25\,°C}$ equal to 9.6-9.8. This result, raised the question of the ODA behavior in steam generators where such temperatures are usual.

Conclusions

The use of FFA is a possible alternative to improve conservation of secondary circuit materials during layup/shutdown periods of units. ODA is a well-known FFA that can be used to hinder magnetite depositions and decrease corrosion rates of carbon steel and low alloyed steel. Even though ODA based conservation appears promising, numerous questions still persist in particular its behavior in the secondary circuit conditions of PWRs. The results presented here helped to have a better understanding of the ODA behavior in specific studied conditions.

First, the water/steam distribution behavior of ODA as a function of the temperature was investigated. Then, the deposition of ODA on carbon steel in particular laboratory conditions was performed by mean of an autoclave at 120 °C, 220 °C and 275 °C. The presence of ODA on the carbon steel surface treated at 120 °C and at 220 °C was confirmed by surface observations and EIS measurements. In the case of the carbon steel sample treated at 275 °C with and without ODA, the contact angle measurement did not show a significant difference to confirm the presence of an organic film. The surface morphology was similar for both samples with and without ODA. The EIS measurements show a slight difference in the electrochemical response for the ODA treated sample at 275 °C during 2 h that could not be attributed to a covering film. In parallel, a study of the kinetics of ODA degradation at 275 °C revealed a degradation of more than 80 % of this product in less than 6 hours. All of these results provide a range of elements in favor of the absence of ODA in SGs, only ODA by-products could remain. More investigations are necessary to determine ODA behavior in all the secondary circuit conditions.

The formation and the characterization of an ODA film formed at low temperature has been recently studied [16]. This study and the present paper provide important elements for the understanding of ODA behavior versus temperature. However, several other key parameters will be determinant on ODA behavior in the secondary circuit conditions: the concentration, the fluid velocity, pH and the nature and morphology of the substrate. In addition, it will be necessary to determine the behavior of ODA degradation products. To go ahead in predicting the conditions of an effective inhibition of the corrosion by ODA in the secondary circuit, the next step will be to determine the impact of each parameters on the characteristics and the effectiveness of the film.

References

[1] I. Betova, M. Bojinov, T. Saario, Film-forming amines in steam / water cycles – structure, properties, and influence on corrosion, VTT. VTT-R-0323 (2014) 1–41.

[2] C.W. Turner, L. Case, Fouling of nuclear steam generators : fundamental studies, operating experience and remedial measures using chemical additives, AECL Nucl. Rev. 2 (2013) 61–88.

[3] Technical guidance document: Application of film-forming amines in fossil, combined cycle, and biomass power plants, IAPWS. (2016).

[4] Q.-Q. Liao, G.-D. Zhou, H.-H. Ge, L.-M. Qi, Characterisation of surface film on iron samples treated with octadecylamine, Corros. Eng. Sci. Technol. 42 (2007) 102–105.

[5] H.-H. Ge, G.-D. Zhou, Q.-Q. Liao, Y.G. Lee, B.H. Loo, A study of anti-corrosion behavior of octadecylamine-treated iron samples, Appl. Surf. Sci. 156 (2000) 39–46.

[6] R. Wagner, E. Czempik, Preservation of boilers and turbines with the surface active substance octadecylamine (ODA), VGB PowerTech J. 2014 (2014) 2–5.

[7] E. V Chernyshev, E.N. Veprov, V.A. Petrov, S.L. Bogdanov, T.Y. Levina, T.I. Petrova, V.I. Kashinskii, A.A. Zonov, A.E. Verkhovskii, Increasing the corrosion resistance of equipment due to the use of film-forming amines, Power Technol. Eng. 40 (2006) 34–37.

[8] A. V. Kurshakov, A. V. Ryzhenkov, A.A. Bodrov, O. V. Ryzhenkov, A.A. Patakin, E.F. Chernov, Heat transfer enhancement in steam-turbine condensers with the use of surface-active substances, Therm. Eng. 61 (2014) 785–789.

[9] W. Hater, D. Olivet, N. Rudschützky, The chemistry and properties of organic boiler feedwater additives based on film-forming amines and their use in steam generators, Powerpl. Chem. 11 (2009) 90–96.

[10] K. Sipilä, T. Saario, Effect of octadecylamine on carbon steel corrosion under PWR secondary side conditions, VTT. (2014) 1–16.

[11] E. Jäppinen, T. Ikäläinen, S. Järvimäki, T. Saario, K. Sipilä, M. Bojinov, Corrosion Behavior of Carbon Steel Coated with Octadecylamine in the Secondary Circuit of a Pressurized Water Reactor, 26 (2017) 6037–6046.

[12] J.J. Benítez, M.A. San-Miguel, S. Domínguez-Meister, J.A. Heredia-Guerrero, M. Salmeron, Structure and chemical state of octadecylamine self-assembled monolayers on mica, J. Phys. Chem. C. 115 (2011) 19716–19723.

[13] U. Ramminger, S. Hoffmann-Wankeri, J. Fandrich, The application of film-forming amines in secondary side chemistry treatments of NPPs, NPC. (2012) O46-167.

[14] B. Hirschorn, M.E. Orazem, B. Tribollet, V. Vivier, I. Frateur, M. Musiani, Constant-Phase-Element Behavior Caused by Resistivity Distributions in Films. II: Applications, J. Electrochem. Soc. 157 (2010) C458.

[15] B. Hirschorn, M.E. Orazem, B. Tribollet, V. Vivier, I. Frateur, M. Musiani, Constant-Phase-Element Behavior Caused by Resistivity Distributions in Films. I: Theory, J. Electrochem. Soc. 157 (2010) C452.

[16] J. Baux, N. Caussé, J. Esvan, S. Delaunay, J. Tireau, M. Roy, D. You, N. Pébère, Impedance analysis of film-forming amines for the corrosion protection of a carbon steel, Electrochim. Acta. 283 (2018) 699–707.

[17] D.R. Lide, CRC Handbook of chemistry and physics, 84th edition, 2003.